Biochimica et Biophysica Acta 1838 (2014) 2280–2288

Contents lists available at ScienceDirect

Biochimica et Biophysica Acta

journal homepage: www.elsevier.com/locate/bbamem

How reliable are molecular dynamics simulations of membrane active antimicrobial peptides?☆

Yukun Wang [a,b], Tangzheng Zhao [a,b], Dongqing Wei [a,b,*], Erik Strandberg [c], Anne S. Ulrich [c,d], Jakob P. Ulmschneider [e,f,*]

[a] The State Key Laboratory of Microbial Metabolism and College of Life Sciences and Biotechnology, Shanghai Jiao Tong University, Shanghai 200240, China
[b] College of Life Sciences and Biotechnology, Shanghai Jiao Tong University, Shanghai 200240, China
[c] Institute of Biological Interfaces (IBG-2), Karlsruhe Institute of Technology, P.O.B. 3640, 76021 Karlsruhe, Germany
[d] Institute of Organic Chemistry, Karlsruhe Institute of Technology, Fritz-Haber Weg 6, 76131 Karlsruhe, Germany
[e] Department of Physics, Shanghai Jiao Tong University, Shanghai 200240, China
[f] The Institute of Natural Sciences, Shanghai Jiao Tong University, Shanghai 200240, China

ARTICLE INFO

Article history:
Received 20 December 2013
Received in revised form 7 March 2014
Accepted 10 April 2014
Available online 18 April 2014

Keywords:
Antimicrobial peptide PGLa
BP100
Maculatin
Melittin
Lipid bilayer membrane
MD force field

ABSTRACT

Membrane-active antimicrobial peptides (AMPs) are challenging to study experimentally, but relatively easy to investigate using molecular dynamics (MD) computer simulations. For this reason, a large number of MD studies of AMPs have been reported over recent years. Yet relatively little effort has focused on the validity of such simulations. Are these results reliable, and do they agree with what is known experimentally? And how much meaningful information can be obtained? To answer these questions, we demonstrate here some of the requirements and limitations of running MD simulations for several common AMPs: PGLa, melittin, maculatin and BP100. The two most important findings are: (a) simulation results depend strongly on force field parameters, making experimental verification of the simulations obligatory, and (b) slow orientational and conformational fluctuations mean that much longer sampling timescales (multi-μs) are needed if quantitative agreement between simulation averages and experimental data is to be achieved. This article is part of a Special Issue entitled: Interfacially Active Peptides and Proteins. Guest Editors: William C. Wimley and Kalina Hristova.

1. Introduction

Membrane-active antimicrobial peptides (AMPs) are found in many organisms and are currently of major pharmaceutical interest as a potential source of new antibiotics against increasingly common multiresistant pathogens [1,2]. Most of these peptides kill bacteria by physically interacting with and disrupting their cell membranes. The exact molecular mechanism concerned is not fully understood at present, with a large number of models proposed over the last decades [3]. Because it is experimentally challenging to study these highly mobile peptides in membranes, molecular dynamics (MD) simulations have been proposed as an alternative. Over the last years, countless such simulations have been presented on a large number of AMPs and related cell-penetrating peptides [4,5]. Because the results of these simulations have been almost as diverse as the mechanisms proposed, the question arises as to how accurate MD actually is and whether these results can be trusted. Interestingly, there is relatively little information on this issue to date. Most MD studies of membrane-active peptides lack any but the most basic verification versus experimental data, so the results have to be taken 'as is'. Previously, in the absence of any quantitative experimental measurements, this situation may have been acceptable. However, considerable progress has been made in recent years to obtain highly accurate information on AMPs and other membrane-active peptides from methods such as oriented circular dichroism (OCD) [6] and solid state NMR [7,8]. Many of these experiments unfortunately say little about the transition state for pore formation and only give information on the more populous ground states. However, they nevertheless provide a valuable benchmark for comparison to MD simulations.

In this short report, we highlight some of the problems of MD simulations of AMPs and how to avoid them. In particular, we show that the results depend vitally on a correct force field parameter balance and on achieving long enough sampling times. Otherwise, MD can yield results that contradict what has been measured experimentally. We do not perform a generic force field comparison here, but focus exclusively on the subject of peptides in membranes. Ultimately, only a combined experimental/computational approach will allow identifying the specific physicochemical properties that lead to antimicrobial function, and thus allow to predict and to improve the therapeutic impact of new AMP sequences.

☆ This article is part of a Special Issue entitled: Interfacially Active Peptides and Proteins. Guest Editors: William C. Wimley and Kalina Hristova.

* Corresponding authors.
E-mail addresses: dqwei@sjtu.edu.cn (D. Wei), jakob@sjtu.edu.cn (J.P. Ulmschneider).

http://dx.doi.org/10.1016/j.bbamem.2014.04.009
0005-2736/

2. Methods

All simulations were performed and analyzed using GROMACS version 4.6.3 (www.gromacs.org) [9] and HIPPO beta (www.biowerkzeug.com), using the CHARMM27 force field [10], the OPLS-AA force field [11], the GROMOS96-53a6 force field [12], and the TIP3P water [13]. CHARMM36 all-atom lipid parameters were used [14], and united atom lipid parameters were taken from Ulmschneider and Ulmschneider [15], and Berger et al. [16]. Electrostatic interactions were computed using particle-mesh-Ewald (PME), and a cut-off of 10 Å was used for the van der Waals interactions. Bonds involving hydrogen atoms were restrained using LINCS [17]. Simulations were run with a 2 fs time-step, and neighbor lists were updated every 5 steps. All simulations were performed in the NPT ensemble, with water, lipids, and the protein coupled separately to a heat bath with T = 35 °C and a time constant $\tau_T = 0.1$ ps using weak temperature coupling [18]. Atmospheric pressure of 1 bar was maintained using weak semi-isotropic pressure coupling with compressibility $\kappa_z = \kappa_{xy} = 4.6 \cdot 10^{-5}$ bar^{-1} and time constant $\tau_P = 1$ ps [19]. All peptides were constructed as ideal α-helices and inserted into a preformed lipid bilayer made up of 58 DMPC lipids and ~30 water molecules per lipids, as described previously [20]. The 1 μs PGLa dimer simulation at 60 °C was performed on the Anton machine at Pittsburg Supercomputing Center, all other simulations (cumulative time of 37 μs) were performed on conventional clusters. For all quantities, the standard deviation of the mean was calculated by block averaging over 10 blocks, and these are plotted as error bars.

To compare with solid state NMR data of a selectively labeled peptide embedded in a macroscopically oriented membrane sample, the corresponding ^{2}H quadrupolar splitting or ^{19}F dipolar coupling was obtained from the simulations by calculating the local bond order parameter S_{CD}:

$$S_{CD} = \left\langle 1/2 \quad 3\cos^2\theta - 1 \right\rangle.$$

Here, the angle θ is between the C_α and C_β bonds of the labeled residue and the membrane normal, which is parallel to the magnetic field (*z*-direction).

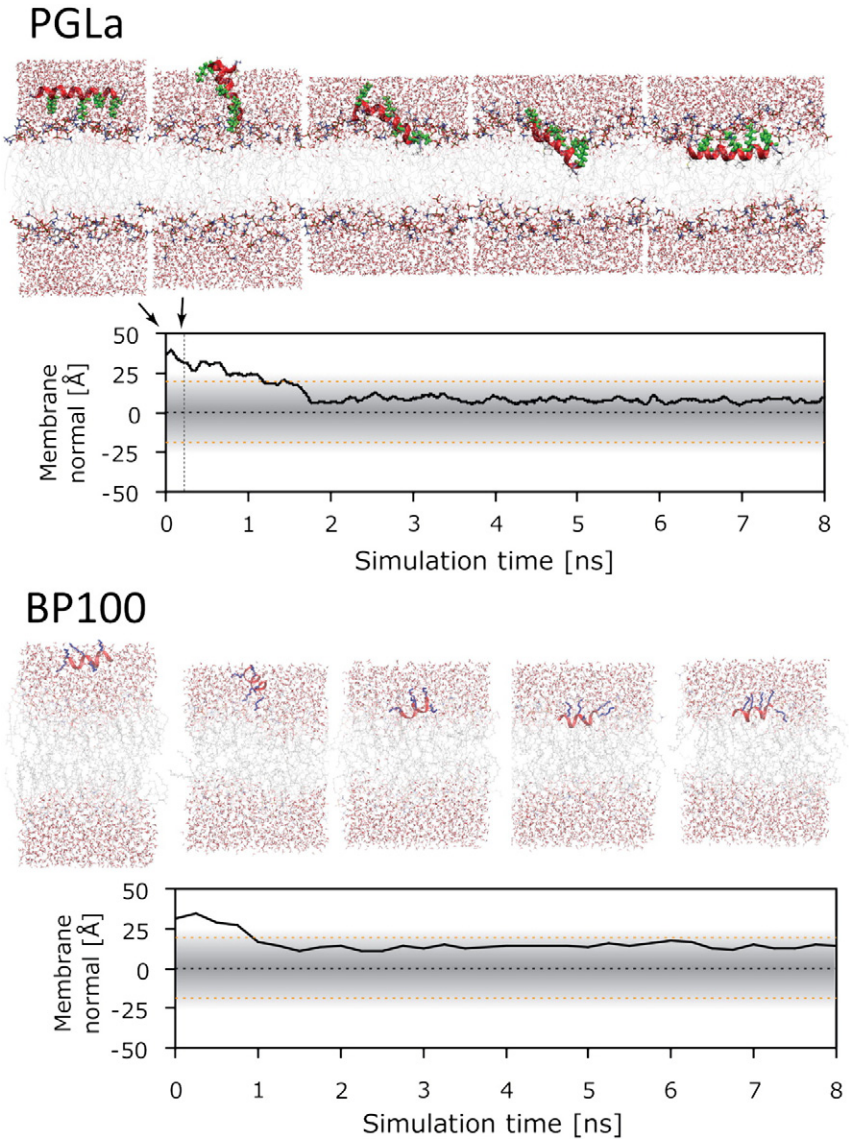

Fig. 1. Two examples of our rapid bilayer insertion simulations, for PGLa (top) and BP100 (bottom). All peptides are initially placed into the solvent, ~40 Å away from the membrane center. The peptides are helically restrained, and the simulation temperature is increased to 90 °C. Rapid insertion is seen during the first 2 ns, and the peptides adopt stable inserted surface (S) states, with the charged sidechains pointing upwards into the bilayer interface. No further transitions occur. The final state of the high-temperature simulations is then used as the starting point for subsequent simulations at room temperature. The approach is completely unbiased, and always yields the same S-state: for example, it plays no role whether the amphipathic peptides initially point their charged sidechains towards the membrane (PGLa simulation, green residues), or away (BP100 simulation, blue residues).

The ^{2}H quadrupolar splitting of an Ala-d_3 label was obtained from

$$\Delta\nu_q = (3/2)Q_{CC}S_{CD} = 42\,\text{kHz}\ S_{CD}$$

where the quadrupolar coupling constant Q_{CC} = 167 kHz for a C–D bond [21], and a factor 1/3 comes from the fast rotation of the CD_3-group around the C_α–C_β bond. The ^{19}F-^{19}F dipolar coupling of a CF_3-group (as for example in CF_3-Bpg, 3-(trifluoromethyl)-L-bicyclopent-[1.1.1]-1-ylglycine [22]) was obtained from

$$\Delta d = 17.0\,\text{kHz}\ S_{CD}$$

where the maximum dipolar coupling between ^{19}F atoms within the CF_3-group used here is an average value obtained from various CF_3-labeled amino acids [23,24]. The quadrupolar splittings and dipolar

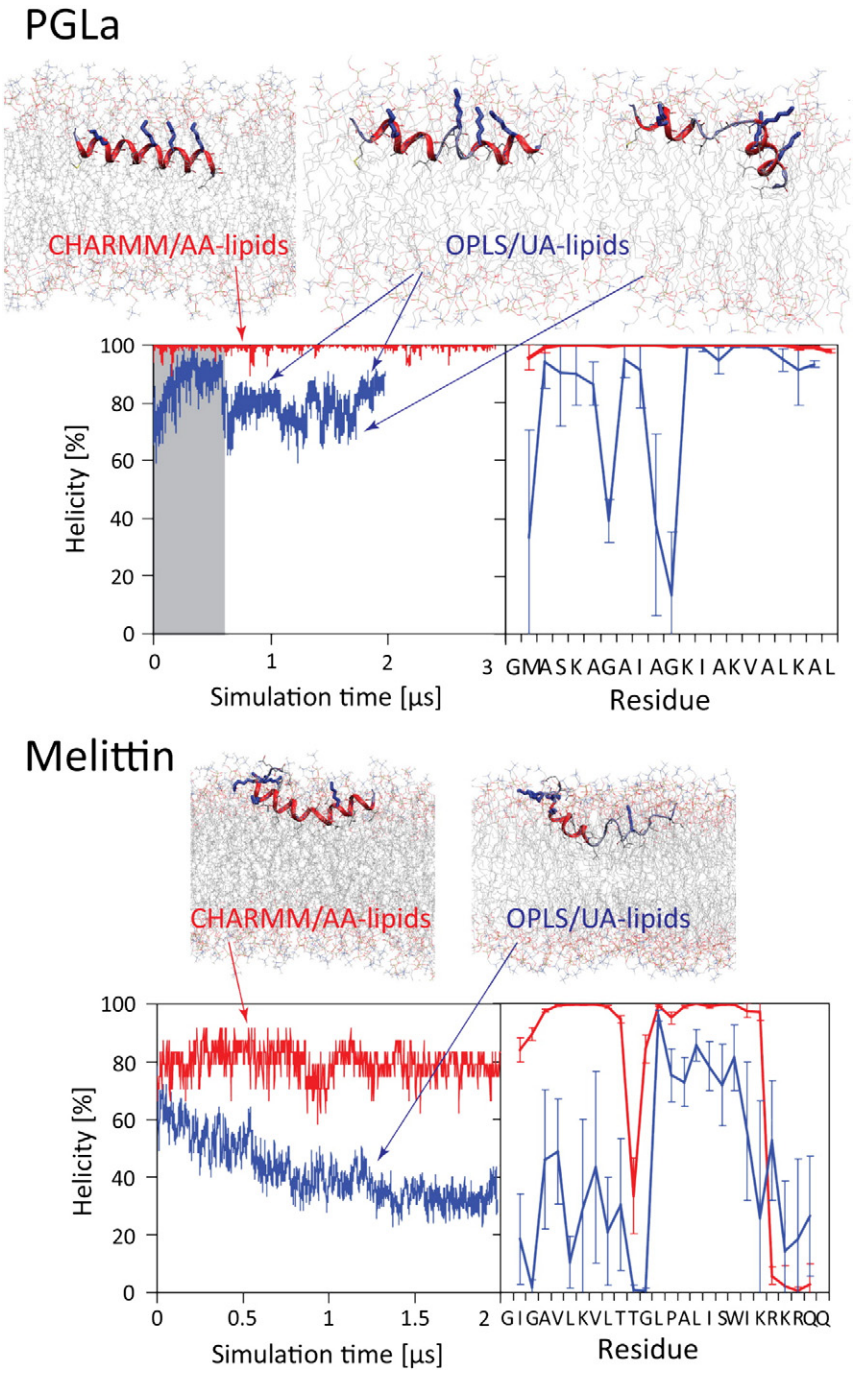

Fig. 2. Secondary structure of two antimicrobial peptides, PGLa (top) and melittin (bottom), in the surface-bound (S-)state. The MD simulations started from full α-helices in the S-state and were run using two different force fields. The overall helicity (left panels) and the helicity per residue (right panels) are shown. When using OPLS with united atom lipids (blue curves), the peptides are substantially less stable than with CHARMM and all-atom lipids (red curves), an effect that was not previously observed for many hydrophobic sequences. Unfolding is a slow process, visible only on the μs time scale: the first unfolding in the central stretch of PGLa occurs only after 600 ns (gray shaded area). The results reveal the subtle equilibrium that needs to be captured to model the complex interactions of amphipathic peptides in the charged and complex bilayer interfaces.

couplings both from NMR experiments and from MD simulations can be fitted with a theoretical model using a procedure described previously [25].

3. Results

3.1. Monomeric surface-bound state

We first investigated the equilibrium of monomeric AMPs at low peptide-to-lipid ratios (P/L), under which the peptides are not expected to exist in any oligomeric state. Given their amphipathic structure, there is usually only one surface-bound (S-)state, where the peptide is inserted with its axis perpendicular to the membrane normal and the charged sidechains pointing upward into the bilayer interface. This state can be rapidly predicted by using unbiased insertion simulations at elevated temperatures (Fig. 1) [20]. The last structure from these simulations is then used as the starting point for the equilibrium simulations at physiological temperature. Fig. 2 shows the results for two representative peptides, PGLa from the African frog *Xenopus laevis* (GMASKAGAIAGKIAKVALKAL-NH_2) [26–28] and melittin (GIGA VLKVLTTGLPALISWIKRKRQQ). Starting from a completely helical structure, both were simulated at the experimental temperature (T = 35 °C) for 2–3 μs, using two different protein force fields (OPLS vs. CHARMM) with different lipid parameters (united atom lipids vs. all-atom lipids). The outcome of these simulations is quite different: in general, the CHARMM/AA-lipid (II) results are much more helical than the OPLS/UA-lipid runs (I). For PGLa, the CHARMM simulation shows a full α-helix, but only ~73% helicity in the OPLS simulation. Several perturbed helical states can be seen (top panels), indicating that the helix is destabilized at the two glycine positions G7 and G11, where the backbone hydrogen bonds are open to polar interfacial groups and water molecules.

The difference is even more dramatic for melittin. Due to a central proline, both simulations show a pronounced kink in the middle of the peptide, and an unstructured (highly charged) C-terminus. However, for OPLS/UA-lipids, there is a slow unfolding of the entire N-terminal half over the course of 2 μs, whereas the CHARMM/AA-lipid simulation predicts a much more helical structure (78%). For both peptides, unfolding is thus a slow process. For example, the first central backbone hydrogen bond in PGLa breaks after 600 ns (OPLS/UA-lipids). Unfolding of melittin takes the full 2 μs. Hence, these long-scale transitions have not been observed in many earlier simulation studies of AMPs where timescales of only 100–200 ns were used. Of course, there is the possibility that ultimately, also the CHARMM/AA-lipid simulation could yield unfolded structures, only taking much longer to do so. We have shown however, that no unfolding of melittin is observed during 17 μs in such simulations [29]. We thus consider that the CHARMM/AA-lipid results converged.

So which simulation result is correct? A good way to answer this question is to compare the MD models with experimental data. Numerous techniques have been used to determine the structure of melittin in the membrane interface, suggesting 70–85% average helicity [30–34]. The unfolding observed in Fig. 2 is inconsistent with this. For PGLa, very accurate information comes from solid state NMR. Measurements from Ala-d_3-labeled PGLa in DMPC at P/L = 1:200 [35] are shown in Fig. 3. These experiments suggest an almost fully folded peptide, with some instability only in the C-terminal region of PGLa (residues A17 to A20), but with an ideal helix from residues A6 to V16 [35]. A comparison of the simulated and experimental quadrupolar splittings $|\Delta\nu_q|$ reveals that the more helical simulations fit much better to the experiments (Fig. 3). Both the helix tilt and the azimuthal rotation angles of the CHARMM/AA-lipid simulations are very close to the NMR results (indicated by a red dot). Overall, this comparison strongly suggests that the unfolding observed for PGLa in MD using OPLS/UA-lipids is erroneous, similar to the melittin result.

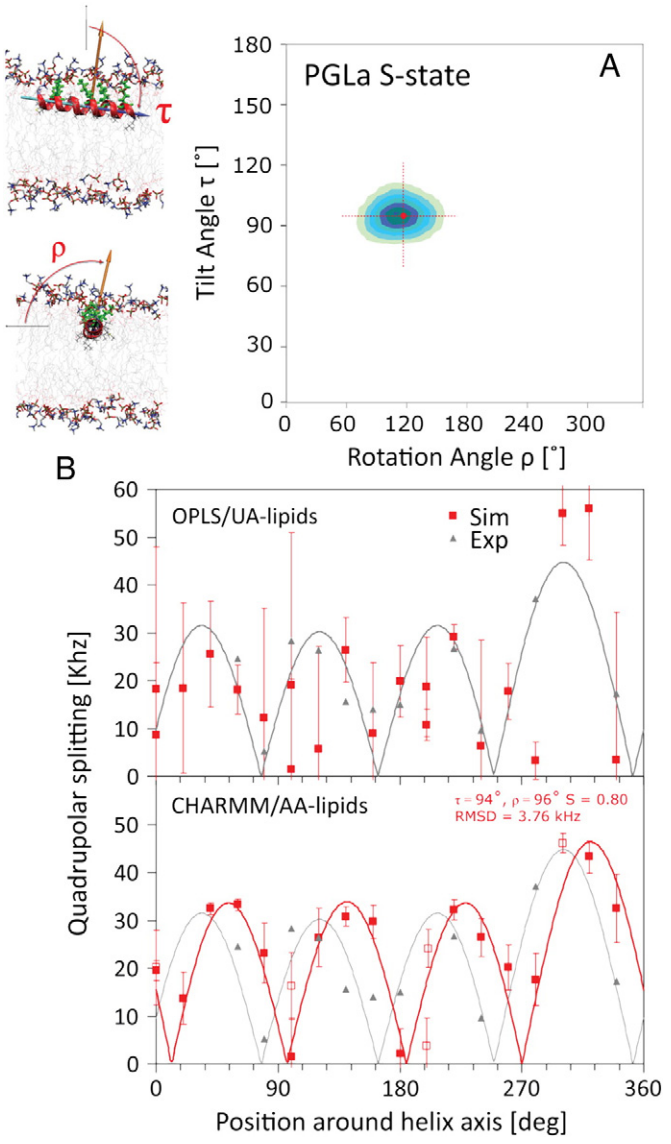

Fig. 3. Solid state NMR is an ideal method to validate the results of MD simulations of AMPs. (A) Orientational histogram (tilt angle τ and azimuthal rotation angle ρ) of PGLa in the S-state averaged over a 3 μs MD run. The average is very close to the NMR results (indicated by a red dot) of $\tau \approx 95°$ and $\rho \approx 116°$. (B) Quadrupolar splittings $|\Delta\nu_q|$ of all residues averaged over the MD simulations (red squares), as compared to solid state NMR measurements of Ala-d_3-labeled PGLa in a DMPC bilayer at P/L = 1:200 (gray triangles) [35]. The curves show the best fit to a helical wave. The unfolding of PGLa in the OPLS simulation results in a large spread of $|\Delta\nu_q|$ values, and the match to NMR is poor. A fit close to the experimental results is obtained for the CHARMM force field in which the peptide remains folded. These results suggest that PGLa is fully helical, and that the unfolding observed in MD is erroneous. Error bars $\sigma^{\text{mean}}_{|\Delta\nu q|}$ are obtained from block averaging.

3.2. Time-scale of folding transitions

Ideally, we could compare force field parameters conveniently the way we have just shown. However, fully folded α-helices were the starting structures in these simulations. In contrast, when the simulations are initiated from coiled or partly folded conformations, the times to reach equilibrium can be very long. We illustrate this for the case of maculatin 1.1 (GLFGVLAKVAAHVVPAIAEHF-NH_2), a cationic AMP isolated from the skin secretions of the frog species *Litoria genimaculata* [36]. Two peptides were studied, with one placed in each bilayer leaflet, and starting from different coiled and partially folded α-helices. In addition to the two force fields used above, we also added simulations using GROMOS96-53a6/UA-lipids. The results are

shown in Fig. 4. Clearly, the simulations are not yet converged on the 2 μs timescale, with the two peptides sampling widely different conformations in each bilayer leaflet. The results also depend strongly on the choice of force field. Unless the two peptides in each simulation reach the same equilibrium, it is unlikely that reliable results can be extracted from such simulations, nor can a decision be made as to which force field performs best. It is obvious that modeling interfacial folding equilibria of AMPs require much longer sampling times than 2 μs, and that simulations shorter than this (unfortunately the case for most studies) appear to be unreliable.

3.3. Long-scale transitions

If a parameter set is found that accurately reproduces the average secondary structure of an AMP, there will still be long-scale transitions in its orientation in the membrane, some of which are related to specific backbone hydrogen bonds breaking or forming on the multi-μs timescale. We can illustrate this using the particularly intriguing peptide BP100, a multifunctional membrane-active sequence with a high antimicrobial activity [37] and an excellent cell-penetrating activity [38]. It carries 6 positive charges and forms an amphiphilic α-helix, similar to other AMPs. However, BP100 is very short, with only 11 amino acids (KKLFKKILKYL-NH_2), and thus cannot form membrane-spanning pores as proposed for longer peptides. We performed MD simulation of BP100 in DMPC bilayers at 35 °C in the surface-bound S-state (Fig. 5), using the CHARMM/AA-lipid force field. The peptide started from a fully helical conformation, an assumption supported by circular dichroism (CD) data that suggests BP100 is predominantly α-helical (61%) in the presence of DMPC/DPMG (3:1) [39]. One of the first surprises was that the peptide can tilt away far from the S-state, by deeply inserting the C-terminus, with a tilt angle of $\tau > 150°$. The tilt is also widely spread ($\pm 14°$), indicating that the peptide is highly mobile. Over 1.5 μs, an average of $\tau = 109°$ was obtained, which is about 40° less than the nominal best-fit tilt angle extracted from the ^{19}F-NMR data (Fig. 6), but in good agreement with the range around $\tau \approx 110°$ as concluded from a combined ^{19}F-NMR/^{15}N-NMR/OCD analysis [39]. In the MD simulations, however, the N-terminal lysines unfolded after 1.5 μs, resulting in a pronounced downshift of the tilt angle. For the remaining simulation time,

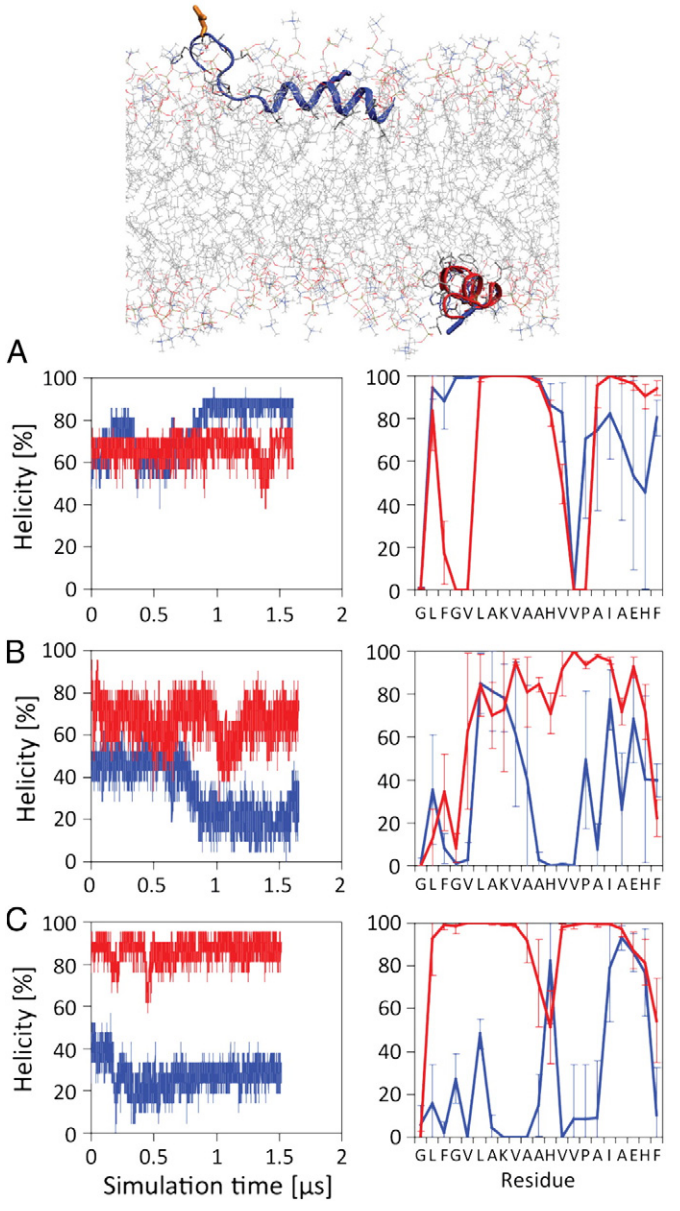

Fig. 4. Helicity of monomeric surface-bound maculatin 1.1 observed in MD simulations in POPC bilayers at 35 °C. Three different force fields were used: CHARMM/AA-lipids (A), OPLS-AA/UA-lipids (B), and GROMOS96-53a6/UA-lipids (C). The simulations started from a mostly folded (red) and one coiled peptide structure (blue). Results vary significantly both between the two peptides and between the different force fields. For a reliable estimate of the helicity of maculatin, much longer simulations would be needed.

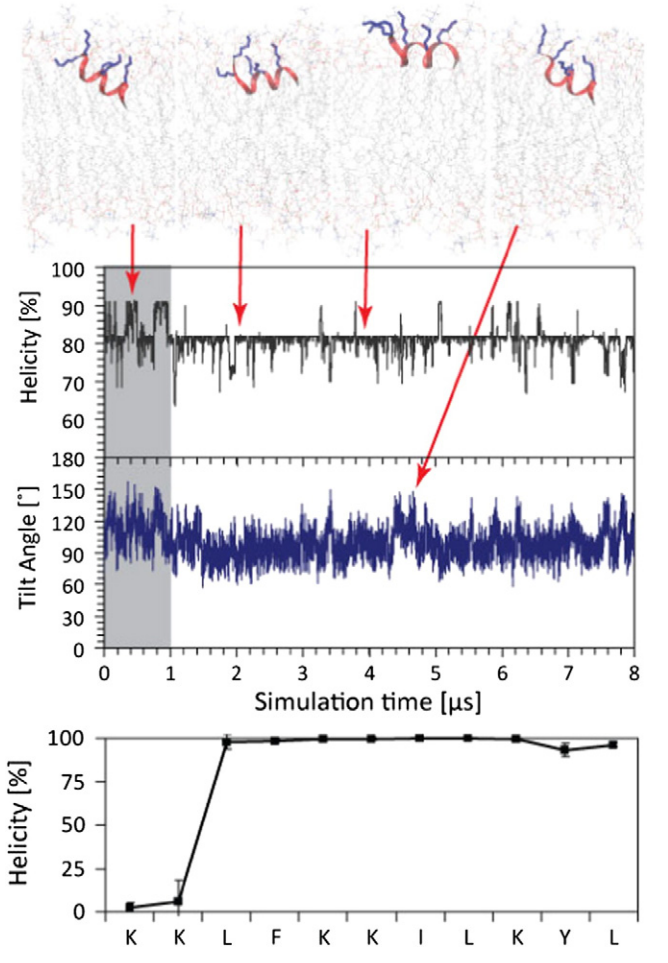

Fig. 5. Orientation and structures observed in a 8 μs MD simulation of BP100 in the S-state of BP100 in a DMPC bilayer at 35 °C. The peptide is initially fully helical. Long-scale transitions of peptide tilt angle are visible, occurring on timescales >1 μs. After 1.5 μs, the N-terminus unfolds, resulting in a significantly reduced tilt angle. Refolding of the N-terminus occurs only very rarely, and it remains on average unfolded (lower panel: average helicity per residue). The equilibrium orientation of BP100 is almost flat, with $\tau = 97° \pm 4°$, but strongly tilted orientations (up to 130°) also occur frequently.

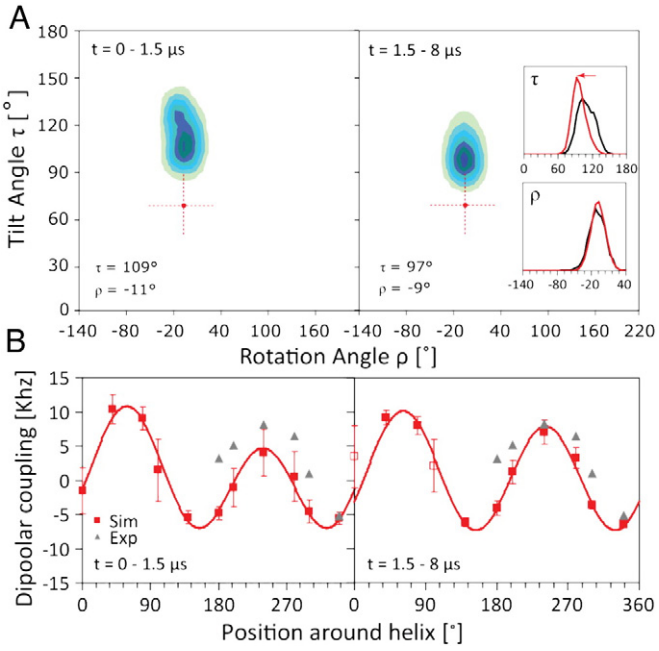

Fig. 6. Time-averaged orientation of BP100 in a DMPC bilayer in the S-state. (A) 2D histograms as a function of the peptide tilt (τ) and azimuthal rotation (ρ) angles. The rotation angle ρ is defined with respect to the C_α atom on Lys 1. The left panel shows the results for the first 1.5 μs, before the N-terminus starts to unfold. The right panel shows the remaining 6.5 μs. The downshift of the tilt angle after 1.5 μs can be seen, while the rotation angle does not change much (insets: histograms of τ and ρ averaged over the simulations, 0–1.5 μs in black, >1.5 μs in red). The nominal best-fit ^{19}F-NMR results are indicated by a red dot ($\tau \approx 70°$ and $\rho \approx -10°$). (B) Dipolar couplings of all residues averaged over the MD simulations (red squares), as compared to couplings from ^{19}F-NMR data of BP100 in DMPC/DMPG (3:1) bilayers at P/L = 1:100 (gray triangles) [39]. The curves show the best fit to a helical wave. The corresponding reduction in tilt angle results in a markedly better match of the MD results (right panel) to the NMR data compared to the first 1.5 μs (left panel), although there is still a 25° tilt angle difference between MD and NMR. These results show how long-scale orientational transitions strongly influence the accuracy of the agreement between simulation and experiment. Error bars $\sigma_{\Delta d}^{mean}$ are obtained from block averaging.

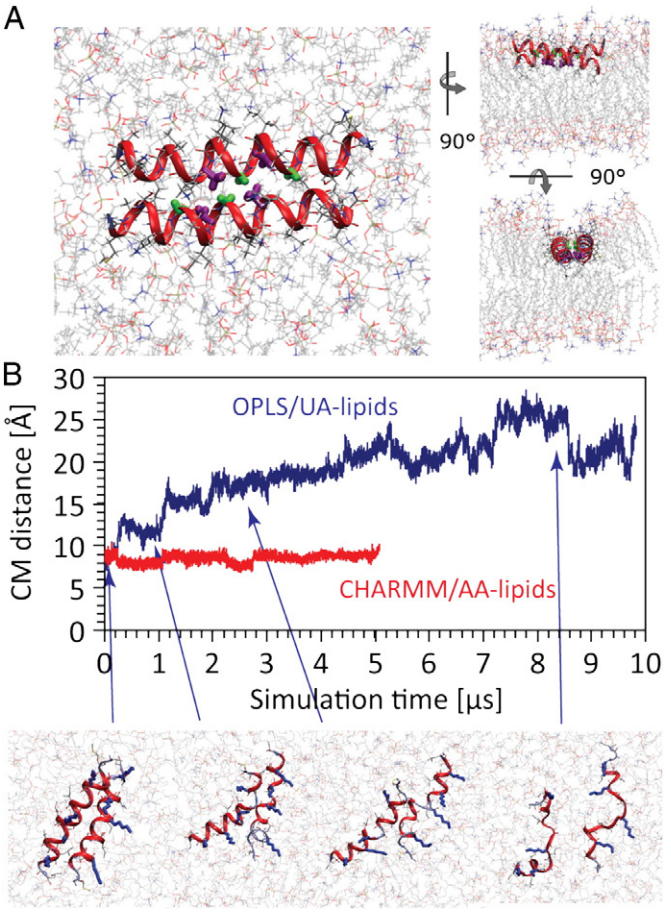

Fig. 7. Example of a putative dimeric structure of PGLa. (A) This particular antiparallel arrangement is stabilized by a dimerization interface made up of the small central residues G11 and G7 (green) and A10 and A14 (purple), resulting in a highly packed, interlocked dimer. (B) Helix–helix center of mass distance as a function of simulation time during MD simulations of the PGLa dimer structure in DMPC bilayers at 35 °C. The stability of the dimer on the μs time-scale depends strongly on the chosen force field parameters. A breakup of the dimer is observed for OPLS/UA-lipids after 250 ns, whereas the dimer is completely stable in the CHARMM/AA-lipid runs.

the average was $\tau = 97°$, as the unfolded lysines at positions 1 and 2 did not allow the peptide to tilt as strongly as before. The average helicity over the second phase was 81%, a bit more than for the wild type peptide, but right in the range of the 77–87% obtained by CD for the CF_3-Bpg labeled analogs used in the NMR studies [39]. The unfolding transition is found to be crucial in improving the accuracy of the simulation results when compared to NMR, as can be seen in Fig. 6. The high tilt angle in the first 1.5 μs is clearly an artifact of the initial simulation conditions (e.g. full helix). In the lower panels of Fig. 6, we directly compare the dipolar couplings obtained from MD and those from ^{19}F-NMR data of BP100 in DMPC/DMPG (3:1) bilayers at P/L = 1:100. The match in the second simulation phase >1.5 μs is significantly better than the one for the first 1.5 μs. These results demonstrate that very long sampling times are essential for a quantitative match between simulations and experiments. Otherwise, the results from MD can strongly depend on initial conditions (here: initial full helix). But even after the unfolding transition at 1.5 μs, the tilt angle of BP100 is seen to undergo large transitions on the time-scale of many microseconds (Fig. 5), which also has a pronounced effect on the solid state NMR data analysis [40]. It is thus unlikely that MD simulations shorter than this are suitable for reliable simulation averages to be compared to experiments, in which the sampling time is many orders of magnitude longer still.

3.4. Aggregates and dimers at higher P/L

So far we have looked only at the equilibria of AMPs at low P/L ratios where we assumed the peptides to be surface-bound and monomeric. If we desire to study the various unknown surface-bound aggregates and possibly inserted transmembrane pores formed by these peptides at high P/L, then the accuracy of the simulation model becomes even more important. Unfortunately, there is very little structural experimental data available to guide an MD simulator in this case.

To illustrate the challenge to accurately model interfacial aggregation of AMPs, we have chosen the example of a putative dimer of PGLa (Fig. 7). This structure was suggested by recent solid-state ^{2}H-, ^{15}N- and ^{19}F-NMR measurements of PGLa in DMPC. Upon an increase of peptide concentration to P/L = 1:100–1:20 a transition occurred from the monomeric S-state to a tilted "T-state", with $\tau \approx 127°$ [25,35,41,42]. Self-assembly of peptides to dimers is likely the reason for the stepwise change of the NMR splittings with peptide concentration [43]. The T-state was suggested to be an antiparallel dimer due to the presence of a single set of NMR splittings indicating that this dimer must be rotationally symmetric with respect to the membrane normal [41]. Loss of helicity was not observed.

Because ab-initio prediction of such aggregates probably requires milliseconds of simulation time, we chose a different path and assembled candidate dimers using a more rapid protocol in which initial dimers were constructed and picked only if they remained intact (Fig. S1) [20]. The antiparallel arrangement shown in Fig. 7 was found in this way. How reliable is this structure? It can be seen that different force fields again lead to very different results. While the OPLS/UA-

lipid simulations were stable for 250 ns, the dimer slowly disintegrated over the course of the following 4 μs, in a stepwise fashion that also included significant unfolding. In contrast, the dimer was found to be entirely stable in the CHARMM/AA-lipid simulations.

In fact the CHARMM/AA-lipid simulations predict the dimer to be so stable that it is essentially impossible to break. This is illustrated in Fig. 8. We placed 4 dimers in a large DMPC lipid bilayer (288 lipids) and increased the simulation temperature to 60 °C. There was a rapid 2-dimensional diffusion of the dimers in their bilayer leaflet, and fast rotational averaging occurred. However, no dimer broke apart or unfolded. No further surface aggregation was seen; in fact the dimers appeared to avoid each other, with only some occasional close encounters involving the termini. The formation of pores was not observed over the 1 μs of simulation time.

4. Discussion

From our results, there are two clear lessons for MD simulations of AMPs: (a) the simulation results depend strongly on force field parameters, making experimental verification of the simulations obligatory, and (b) slow orientational and conformational fluctuations mean that very long sampling timescales (multi-μs) are needed if quantitative agreement between simulation averages and experimental data is to be achieved. Apparently, the challenge to accurately model AMPs is already tough for the simplest case of monomeric surface-bound (S) states at low peptide-to-lipid ratios. This means that the modeling of much more complex phenomena, such as aggregation and pore formation at high P/L, is unlikely to succeed unless the underlying models have been properly tested and tuned.

It is not clear what causes the large differences observed in our simulation studies. The partial charges of protein backbone groups of OPLS, CHARMM and GROMOS are nearly identical and should lead to the same strength of hydrogen bonds and thus secondary structure. Some incongruencies might be attributed to differences in backbone torsion angles. However, the most obvious culprit is the balance between the lipid and protein force fields. We have simulated OPLS and GROMOS with united atom lipids, but CHARMM with all-atom lipids. This is a major difference. Not only do united atom lipids allow for more protein flexibility – and thus unfolding – but there is also a difference in how deep water molecules penetrate into the interface. The interactions between peptide and lipid atoms in the polar lipid phosphocholine headgroups, as well as the glycerol linker and ester groups, are highly complex and have been the topic of numerous studies. A change from all-atom to united atom lipids almost certainly will shift this balance. Thus, the probable cause for the differences in structural stability of the peptides is not the protein force field per se, but rather the imbalance between lipid and protein force fields. Unfortunately, no OPLS or GROMOS all-atom lipid parameters for DMPC/POPC are available to test this assumption. If correct, this dilemma would affect most of the published simulations of AMPs, which have overwhelmingly been based on united atom lipid force fields (for speed). More studies are clearly necessary to investigate these issues.

Our results mirror earlier observations on hydrophobic WALP peptides (which are of similar length to AMPs) in lipid bilayers, which had shown some unnatural helical unfolding on the μs-scale [15,44–46]. In addition to force field issues, it has also been recently demonstrated that the outcome of simulations of membrane-active peptides is greatly influenced by the choice of the electrostatic long-range models, and by the inclusion or omission of counter-ions [4]. Thus, great care

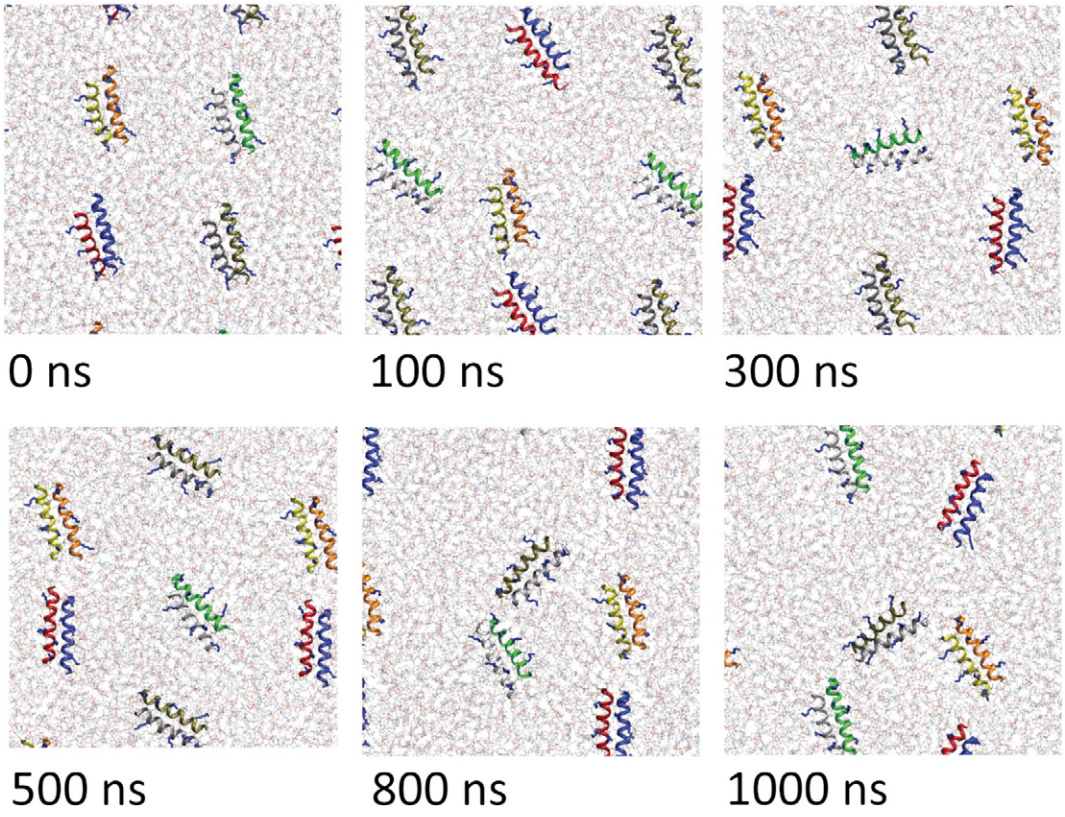

Fig. 8. MD simulation of multiple PGLa antiparallel dimers in a DMPC bilayer. The temperature was raised to 60 °C to increase the speed of orientational sampling. Even at 60 °C, the dimers are completely stable (using the CHARMM/AA-lipid method), and no breakup or unfolding is observed over 1 μs. Rapid translational drift and rotational averaging (around the membrane normal) are observed. However, aggregation does not occur, because either the temperature is too high or the timescale is too short.

must be taken before drawing conclusions from MD simulations of AMPs.

Our second observation is that short MD simulations ($t < 1–2$ μs) are – at best – qualitative. Major transitions in the backbone, sidechain orientations and the overall tilt and azimuthal rotation angles occur on timescales of many μs. A particular illustration of this point was shown in a recently very long 17 μs MD study of melittin in DOPC bilayers [29]. Two peptides were placed on the bilayer interface, one in each leaflet. In one peptide a sudden folding transition occurred at 8 μs, increasing its helicity from 75 to 89% and resulting in very different dominating conformational clusters. Thus, it is still challenging to obtain reliable equilibria from MD, unless the simulations become much longer than the timescale of these sudden events. The biophysical experiments are obviously on much longer timescales, so it is clear that only for very long multi-μs runs there is a chance of a quantitative agreement. Fortunately, much longer simulations can now be run routinely on high performance clusters, or on special hardware such as Anton.

Acknowledgements

This research was supported by a grant from the National Natural Science Foundation of China (BC4190004) and a 1000 young talent grant to J.P.U. and in part by grants from the National High-Tech R&D Program (863 program contract no. 2012AA020307 to D.Q.W.), the National Basic Research Program of China (973 program contract no. 2012CB721000 to D.Q.W.), and the Key Project of Shanghai Science and Technology Commission (contract no. 11JC1406400 to D.Q.W.). Anton computer time was provided by the National Resource for Biomedical Supercomputing and the Pittsburgh Supercomputing Center (through grant PSCA13011P). The Anton machine is supported by NIH grant RC2GM093307 and was generously made available by D.E. Shaw Research. We also acknowledge the DFG-Center for Functional Nanotechnology (project E1.2).

Appendix A. Supplementary data

Supplementary data to this article can be found online at http://dx.doi.org/10.1016/j.bbamem.2014.04.009.

References

[1] R.M. Epand, H.J. Vogel, Diversity of antimicrobial peptides and their mechanisms of action, Biochim. Biophys. Acta (BBA) 1462 (1999) 11–28.
[2] W. van 't Hof, E.C. Veerman, E.J. Helmerhorst, A.V. Amerongen, Antimicrobial peptides: properties and applicability, Biol. Chem. 382 (2001) 597–619.
[3] L.T. Nguyen, E.F. Haney, H.J. Vogel, The expanding scope of antimicrobial peptide structures and their modes of action, Trends Biotechnol. 29 (2011) 464–472.
[4] A.A. Gurtovenko, J. Anwar, I. Vattulainen, Defect-mediated trafficking across cell membranes: insights from in silico modeling, Chem. Rev. 110 (2010) 6077–6103.
[5] G. Bocchinfuso, S. Bobone, C. Mazzuca, A. Palleschi, L. Stella, Fluorescence spectroscopy and molecular dynamics simulations in studies on the mechanism of membrane destabilization by antimicrobial peptides, Cell. Mol. Life Sci. 68 (2011) 2281–2301.
[6] J. Bürck, S. Roth, P. Wadhwani, S. Afonin, N. Kanithasen, E. Strandberg, A.S. Ulrich, Conformation and membrane orientation of amphiphilic helical peptides by oriented circular dichroism, Biophys. J. 95 (2008) 3872–3881.
[7] E. Strandberg, A.S. Ulrich, NMR methods for studying membrane-active antimicrobial peptides, Concepts Magn. Reson. Part A 23A (2004) 89–120.
[8] A.S. Ulrich, Solid state ^{19}F NMR methods for studying biomembranes, Prog. Nucl. Magn. Reson. Spectrosc. 46 (2005) 1–21.
[9] H.J.C. Berendsen, D. van der Spoel, R. van Drunen, GROMACS: a message-passing parallel molecular dynamics implementation, Comp. Phys. Comm. 95 (1995) 43–56.
[10] A.D. MacKerell, D. Bashford, R.L. Dunbrack Bellott, J.D. Evanseck, M.J. Field, S. Fischer, J. Gao, H. Guo, S. Ha, D. Joseph-McCarthy, L. Kuchnir, K. Kuczera, F.T.K. Lau, C. Mattos, S. Michnick, T. Ngo, D.T. Nguyen, B. Prodhom, W.E. Reiher, B. Roux, M. Schlenkrich, J.C. Smith, R. Stote, J. Straub, M. Watanabe, J. Wiórkiewicz-Kuczera, D. Yin, M. Karplus, All-atom empirical potential for molecular modeling and dynamics studies of proteins†, J. Phys. Chem. B 102 (1998) 3586–3616.
[11] W.L. Jorgensen, D.S. Maxwell, J. Tirado-Rives, Development and testing of the OPLS all-atom force field on conformational energetics and properties of organic liquids, J. Am. Chem. Soc. 118 (1996) 11225–11236.
[12] C. Oostenbrink, A. Villa, A.E. Mark, W.F. Van Gunsteren, A biomolecular force field based on the free enthalpy of hydration and solvation: the GROMOS force-field parameter sets 53A5 and 53A6, J. Comput. Chem. 25 (2004) 1656–1676.
[13] W.L. Jorgensen, J. Chandrasekhar, J.D. Madura, R.W. Impey, M.L. Klein, Comparison of simple potential functions for simulating liquid water, J. Chem. Phys. 79 (1983) 926–935.
[14] J.B. Klauda, R.M. Venable, J.A. Freites, J.W. O'Connor, D.J. Tobias, C. Mondragon-Ramirez, I. Vorobyov, A.D. MacKerell, R.W. Pastor, Update of the CHARMM all-atom additive force field for lipids: validation on six lipids types, J. Phys. Chem. B 114 (2010) 7830–7843.
[15] J.P. Ulmschneider, M.B. Ulmschneider, United atom lipids parameters for combination with the optimized potentials for liquid simulations all-atom force field, J. Chem. Theory Comput. 5 (2009) 1803–1813.
[16] O. Berger, O. Edholm, F. Jahnig, Molecular dynamics simulations of a fluid bilayer of dipalmitoylphosphatidycholine at full hydration, constant pressure and constant temperature, Biophys. J. 72 (1997) 2002–2013.
[17] B. Hess, H. Bekker, H.J.C. Berendsen, J.G.E.M. Fraaije, LINCS: a linear constraint solver for molecular simulations, J. Comp. Chem. 18 (1997) 1463–1472.
[18] G. Bussi, D. Donadio, M. Parrinello, Canonical sampling through velocity rescaling, J. Chem. Phys. 126 (2007) 014101.
[19] H.J.C. Berendsen, J.P.M. Postma, W.F. Vangunsteren, A. Dinola, J.R. Haak, Molecular-dynamics with coupling to an external bath, J. Chem. Phys. 81 (1984) 3684–3690.
[20] J.P. Ulmschneider, J.C. Smith, M.B. Ulmschneider, A.S. Ulrich, E. Strandberg, Reorientation and dimerization of the membrane-bound antimicrobial peptide PGLa from microsecond all-atom MD simulations, Biophys. J. 103 (2012) 472–482.
[21] J.H. Davis, The description of membrane lipids conformation, order and dynamics by 2H-NMR, Biochim. Biophys. Acta (BBA) 737 (1983) 117–171.
[22] S. Afonin, P.K. Mikhailiuk, I.V. Komarov, A.S. Ulrich, Evaluating the amino acid CF_3-bicyclopentylglycine as a new label for solid-state ^{19}F-NMR structure analysis of membrane-bound peptides, J. Pept. Sci. 13 (2007) 614–623.
[23] U.H.N. Dürr, S.L. Grage, R. Witter, A.S. Ulrich, Solid state ^{19}F NMR parameters of fluorine-labeled amino acids. Part I: aromatic substituents, J. Magn. Res. 191 (2008) 7–15.
[24] S.L. Grage, U.H.N. Dürr, S. Afonin, P.K. Mikhailiuk, I.V. Komarov, A.S. Ulrich, Solid state 19F NMR parameters of fluorine-labeled amino acids. Part II: aliphatic substituents, J. Magn. Res. 191 (2008) 16–23.
[25] E. Strandberg, P. Wadhwani, P. Tremouilhac, U.H. Dürr, A.S. Ulrich, Solid-state NMR analysis of the PGLa peptide orientation in DMPC bilayers: structural fidelity of ^{2}H-labels versus high sensitivity of ^{19}F-NMR, Biophys. J. 90 (2006) 1676–1686.
[26] W. Hoffmann, K. Richter, G. Kreil, A novel peptide designated PYLa and its precursor as predicted from cloned mRNA of *Xenopus laevis* skin, EMBO J. 2 (1983) 711–714.
[27] K. Richter, H. Aschauer, G. Kreil, Biosynthesis of peptides in the skin of *Xenopus laevis*: isolation of novel peptides predicted from the sequence of cloned cDNAs, Peptides 6 (Suppl. 3) (1985) 17–21.
[28] D. Andreu, H. Aschauer, G. Kreil, R.B. Merrifield, Solid-phase synthesis of PYLa and isolation of its natural counterpart, PGLa [PYLa-(4–24)] from skin secretion of *Xenopus laevis*, Eur. J. Biochem. 149 (1985) 531–535.
[29] M. Andersson, Jakob P. Ulmschneider, Martin B. Ulmschneider, Stephen H. White, Conformational states of melittin at a bilayer interface, Biophys. J. 104 (2013) L12–L14.
[30] A.S. Ladokhin, S.H. White, Folding of amphipathic alpha-helices on membranes: energetics of helix formation by melittin, J. Mol. Biol. 285 (1999) 1363–1369.
[31] C.E. Dempsey, G.S. Butler, Helical structure and orientation of melittin in dispersed phospholipids membranes from amide exchange analysis in situ, Biochemistry 31 (1992) 11973–11977.
[32] H. Vogel, F. Jähnig, The structure of melittin in membranes, Biophys. J. 50 (1986) 573–582.
[33] P.F. Almeida, A. Pokorny, Mechanisms of antimicrobial, cytolytic, and cell-penetrating peptides: from kinetics to thermodynamics, Biochemistry 48 (2009) 8083–8093.
[34] A. Ladokhin, M. Fernández-Vidal, S. White, CD spectroscopy of peptides and proteins bound to large unilamellar vesicles, J. Membr. Biol. 236 (2010) 247–253.
[35] E. Strandberg, P. Tremouilhac, P. Wadhwani, A.S. Ulrich, Synergistic transmembrane insertion of the heterodimeric PGLa/magainin 2 complex studied by solid-state NMR, Biochim. Biophys. Acta (BBA) 1788 (2009) 1667–1679.
[36] T. Rozek, R.J. Waugh, S.T. Steinborner, J.H. Bowie, M.J. Tyler, J.C. Wallace, The maculatin peptides from the skin glands of the tree frog *Litoria genimaculata*: a comparison of the structures and antibacterial activities of maculatin 1.1 and caerin 1.1, J. Pept. Sci. 4 (1998) 111–115.
[37] E. Badosa, R. Ferre, M. Planas, L. Feliu, E. Besalú, J. Cabrefiga, E. Bardají, E. Montesinos, A library of linear undecapeptides with bactericidal activity against phytopathogenic bacteria, Peptides 28 (2007) 2276–2285.
[38] K. Eggenberger, C. Mink, P. Wadhwani, A.S. Ulrich, P. Nick, Using the peptide BP100 as a cell-penetrating tool for the chemical engineering of actin filaments within living plant cells, Chembiochem 12 (2011) 132–137.
[39] P. Wadhwani, E. Strandberg, J. van den Berg, C. Mink, J. Bürck, R. Ciriello, A.S. Ulrich, Dynamical structure of the short multifunctional peptide BP100 in membranes, Biochim. Biophys. Acta (BBA) 1838 (2014) 940–949.
[40] E. Strandberg, S. Esteban-Martín, J. Salgado, A.S. Ulrich, Orientation and dynamics of peptides in membranes calculated from 2H-NMR data, Biophys. J. 96 (2009) 3223–3232.
[41] R.W. Glaser, C. Sachse, U.H.N. Dürr, P. Wadhwani, S. Afonin, E. Strandberg, A.S. Ulrich, Concentration-dependent realignment of the antimicrobial peptide

PGLa in lipids membranes observed by solid-state ^{19}F-NMR, Biophys. J. 88 (2005) 3392–3397.
[42] P. Tremouilhac, E. Strandberg, P. Wadhwani, A.S. Ulrich, Conditions affecting the realignment of the antimicrobial peptide PGLa in membranes as monitored by solid state ^{2}H-NMR, Biochim. Biophys. Acta (BBA) 1758 (2006) 1330–1342.
[43] S. Afonin, S.L. Grage, M. Ieronimo, P. Wadhwani, A.S. Ulrich, Temperature-dependent transmembrane insertion of the amphiphilic peptide PGLa in lipids bilayers observed by solid state ^{19}F NMR spectroscopy, J. Am. Chem. Soc. 130 (2008) 16512–16514.
[44] M.B. Ulmschneider, J.P. Ulmschneider, Folding peptides into lipids bilayer membranes, J. Chem. Theory Comput. 4 (2008) 1807–1809.
[45] J.P. Ulmschneider, J.P.F. Doux, J.A. Killian, J.C. Smith, M.B. Ulmschneider, Peptide partitioning and folding into lipids bilayers, J. Chem. Theory Comput. 5 (2009) 2202–2205.
[46] M.B. Ulmschneider, J.P.F. Doux, J.A. Killian, J. Smith, J.P. Ulmschneider, Mechanism and kinetics of peptide partitioning into membranes, J. Am. Chem. Soc. 132 (2010) 3452–3460.